Current Zoology, 2024, **70**, 596–606
https://doi.org/10.1093/cz/zoad043
Advance access publication 24 September 2023
Original Article

Balancing selection shapes population differentiation of major histocompatibility complex genes in wild golden snub-nosed monkeys

Shixuan Dong[a], Bingyi Zhang[a], Kang Huang[a], Meijing Ying[a], Jibing Yan[a], Fei Niu[a], Hanyu Hu[b], Derek W. Dunn[a], Yi Ren[c], Baoguo Li[a,*] and Pei Zhang[a,*]

[a]Shaanxi Key Laboratory for Animal Conservation, College of Life Sciences, Northwest University, Xi'an 710069, China
[b]Education Department, Xi'an Gaoxin No. 5 High School, Xi'an 710404, China
[c]Shaanxi Key Laboratory for Animal Conservation, Shaanxi Institute of Zoology, Xi'an 710032, China

[*]Address correspondence to Baoguo Li. E-mail: baoguoli@nwu.edu.cn; Pei Zhang. E-mail: peizhang@nwu.edu.cn.
Handling editor: Zhi-Yun Jia

Abstract

Small and isolated populations face several intrinsic risks, such as genetic drift, inbreeding depression, and reduced gene flow. Thus, patterns of genetic diversity and differentiation have become an important focus of conservation genetics research. The golden snub-nosed monkey *Rhinopithecus roxellana*, an endangered species endemic to China, has experienced rapid reduction in population size and severe population fragmentation over the past few decades. We measured the patterns of genetic diversity and population differentiation using both neutral microsatellites and adaptive major histocompatibility complex (MHC) genes in 2 *R. roxellana* populations (DPY and GNG) distributed on the northern and southern slopes of the Qinling Mountains, respectively. Eight MHC-linked haplotypes formed by 5 *DQA1* alleles, 5 *DQB1* alleles, 5 *DRB1* alleles, and 4 *DRB2* alleles were detected in the 2 populations. The larger GNG population showed higher genetic variation for both MHC and microsatellites than the smaller DPY population, suggesting an effect of genetic drift on genetic variation. Genetic differentiation index (F_{ST}) outlier analyses, principal coordinate analysis (PCoA), and inferred population genetic structure showed lower genetic differentiation in the MHC variations than microsatellites, suggesting that pathogen-mediated balancing selection, rather than local adaptation, homogenized the MHC genes of both populations. This study indicates that both balancing selection and genetic drift may shape genetic variation and differentiation in small and fragmented populations.

Key words: balancing selection, genetic diversity, major histocompatibility complex, population differentiation, *Rhinopithecus roxellana*.

In 2021, 38,543 species were classified as being "at some level of risk of extinction," representing 28% of all 138,374 species assessed on the IUCN Red List of Threatened Species (IUCN 2021). Serious factors affecting most endangered species are habitat destruction and fragmentation, resulting in small and isolated populations (Moqanaki and Cushman 2017). Small and isolated populations may experience a reduction of genetic diversity within populations, which may have negative effects. Genetic diversity reduction occurs due to increased rates of genetic drift and inbreeding, and decreased rates of gene flow when populations become small and isolated (Potter et al. 2017; Zhai et al. 2019; Princepe et al. 2022; Weeks et al. 2022). Genetic diversity is closely related to the ability of a population to cope with environmental changes (Hoffman et al. 2020; Manel et al. 2020; Satake et al. 2022). The higher the genetic diversity of a population, the higher the adaptability and flexibility of a population to a changing environment. When habitat fragmentation occurs, small and isolated populations are thus more likely to fall into an extinction spiral amid declining genetic variation (Willi et al. 2006; Nabutanyi and Wittmann 2021). Extinction can occur when population size drops below a specific threshold (Courchamp et al. 2008), which has been shown in several species with population sizes of 50–500 individuals (Courchamp et al. 1999; Wittmann et al. 2018; Wang et al. 2022).

In addition to the effects within individual populations, habitat fragmentation also increases genetic differentiation among populations. This is due to several factors, one being random genetic drift, which may result in different directions of genetic change in each population and thus an overall intensification of differentiation among fragmented populations (Slatkin 1987; Morris et al. 2008; Fitzpatrick et al. 2020). Another factor is limited gene flow among populations. Both natural and anthropogenic geographical barriers such as rivers, roads, and mountain ranges will increase the costs of migration between populations, thus weakening the function of gene flow in maintaining genetic polymorphisms among populations (Kaufmann et al. 2017).

The major histocompatibility complex (MHC) is a multi-gene family that encodes cell surface glycoproteins, which play an important role in the immune system by recognizing foreign antigens and presenting them to T cells, thereby triggering appropriate immune responses (Klein 1987; Ryan and Cobb 2012; He et al. 2022a). MHC genes can be divided into

Received 12 June 2023; accepted 21 September 2023

2 classes, class I and class II, which bind intracellular (such as viruses) and extracellular foreign antigens (such as bacteria and parasites), respectively (Xu et al. 2009; Neefjes et al. 2011; Wolfert and Boons 2013). MHC genes are highly polymorphic, especially at antigen-binding sites (ABSs) (Eizaguirre et al. 2012). Variation in the ABSs of different MHC genes determines the range of antigens that can be recognized and fight off. Therefore, pathogen-driven balancing selection is a major factor shaping MHC polymorphism, which is partially the result of an arms race between pathogens and the host's immune system (Boyd et al. 2021; Paterson et al. 2021; He et al. 2022b). Because MHC genes are subject to selection, these genes are ideal adaptive markers for examining adaptive genetic variation among and within populations. Compared with neutral genes, such as microsatellites (also known as Short Sequence Repeats, SSRs), which are not subject to selection and thus reflect population demographic history (Lan et al. 2019; Shortreed et al. 2020; de Groot et al. 2022), adaptive MHC genes tend to show different levels of genetic diversity and population differentiation due to balancing selection (Lan et al. 2019; Gong et al. 2021).

The golden snub-nosed monkey *Rhinopithecus roxellana* is an endangered primate endemic to China. Although once widely distributed across what is now modern China, *R. roxellana* is currently confined to fragmented mixed forest in 4 provinces (Sichuan, Gansu, Shaanxi, and Hubei) (Li et al. 2002). The population size of *R. roxellana* has decreased significantly over the last 25,000 years (Luo et al. 2012a). In the past 400 years, this decline has accelerated sharply, with most populations in southwestern, eastern, and central China now extinct (Savage and Baker 1996; Li et al. 2002). Due to both ecological and anthropogenic factors, the overall population of *R. roxellana* over the last 40 years has been reduced by approximately 50%, making this species among the most endangered animals in China (Long and Richardson 2021).

Golden snub-nosed monkeys live in a multilevel society (MLS), made up of a breeding band and an all-male band (Qi et al. 2009; Yang et al. 2022). The breeding band is comprised of several one-male units (OMUs), each of which consists of one adult male, multiple adult females, subadult individuals, and infants (Qi et al. 2009). Bachelor males including adult, sub-adult, and juvenile males form an all-male band that either shadows a single or multiple breeding bands (Qi et al. 2014, 2017).

Movement of bachelor males across the landscape, along with their associations with several neighboring breeding bands, provides a mechanism for promoting gene flow and thus maintaining genetic diversity that may counteract the effects of population isolation (Haimoff et al. 1987; Li et al. 2020). However, research at a larger geographical scale has shown that *R. roxellana* in 5 reserves in the Qinling Mountains, Shaanxi Province, are highly structured and form at least 3 distinct subpopulations that concur with major topographical features such as mountain ridges. This suggests that individual dispersal and gene flow among populations is restricted by geographical barriers (Huang et al. 2016) and that gene flow is severely restricted among individuals resident in distant breeding bands. Genetic differentiation will then intensify between populations spaced far apart, assuming they also possess independent local adaptations. On the other hand, balancing selection favoring adaptive genes (e.g., MHC) can reduce population differentiation (Schierup et al. 2000). However, little is known about which effect of balancing selection and local adaptation is acting on the differentiation between *R. roxellana* populations.

We genotyped 20 SSRs and 4 MHC Class II loci (*DQA1*, *DQB1*, *DRB1*, and *DRB2*) in 2 *R. roxellana* populations, one located on the southern and one on the northern slope of the Qinling Mountains. We sought to quantify: (i) the amount of genetic diversity and patterns of genetic differentiation of the 2 populations and (ii) evidence of local adaptation or balancing selection playing a role in any patterns of genetic differentiation between these 2 populations.

Materials and Methods

Study area and sample collection

Field work was conducted on 2 *R. roxellana* populations (DPY: from 2018 to 2021; GNG: from 2012 to 2018) located on 2 slopes of the Qinling Mountains in Shaanxi Province. The DPY population is located in the Guanyinshan National Nature Reserve on the southern slope (107°52'–108°02' E, 33°20'–33°44' N), while the GNG population is in the Zhouzhi National Nature Reserve on the northern slope (108°14'–108°18' E, 33°45'–33°50' N). During the study period, the DPY population composed of a breeding band consisting of 6–12 OMUs (in total 17 OMUs) and an all-male band of between 1 and 13 bachelor males. The GNG population composed of a breeding band of between 11 and 19 OMUs (in total 52 different OMUs) and a single all-male band of between 21 and 40 bachelor males (Qi et al. 2017; Li et al. 2020). A total of 401 biological samples were collected from the 2 study populations (indicated in Figure 1 DPY and GNG; Table 1). All samples were collected non-invasively and procedures complied with the animal welfare laws and constitutions of China.

Hair samples were collected using a short pole with glue at one end so the hair would be removed when a focal animal was touched with the stick and the stick then moved carefully back toward the field-worker. Each hair sample was stored individually with desiccant in a paper envelope. Each fresh fecal sample (<50 g) was placed into a vial with 50 mL DMSO solution (DETs: 20% DMSO, 0.25 M sodium-EDTA, 100 mM Tris–HCl, pH 7.5, and NaCl to saturation) and stored at –20 °C. We defined a fresh fecal sample as one that has been exposed to air for no more than 15 min.

Molecular techniques

DNA extraction

Genomic DNA was extracted from each hair sample according to the Chelex protocol (Chelex 100, Bio-Rad) (Allen et al. 1998). Fecal DNA was extracted using QIAamp DNA Stool Mini Kits (Qiagen, Germany).

SSR genotyping

We measured the genetic variation of 20 SSRs (see Huang et al. 2016). Each sample was genotyped at these SSRs using previously described methods (Huang et al. 2016).

MHC genotyping

We examined exon 2 of 4 MHC loci (*DQA1*, *DQB1*, *DRB1*, and *DRB2*). All 4 loci were amplified with primer pairs used previously (*DQA1*: Zhang et al. 2016; *DQB1*: Qiu et al. 2008; *DRB1* and *DRB2*: Luo and Pan 2013). Genotyping of *DQA1* and *DQB1* loci was conducted by cloning and

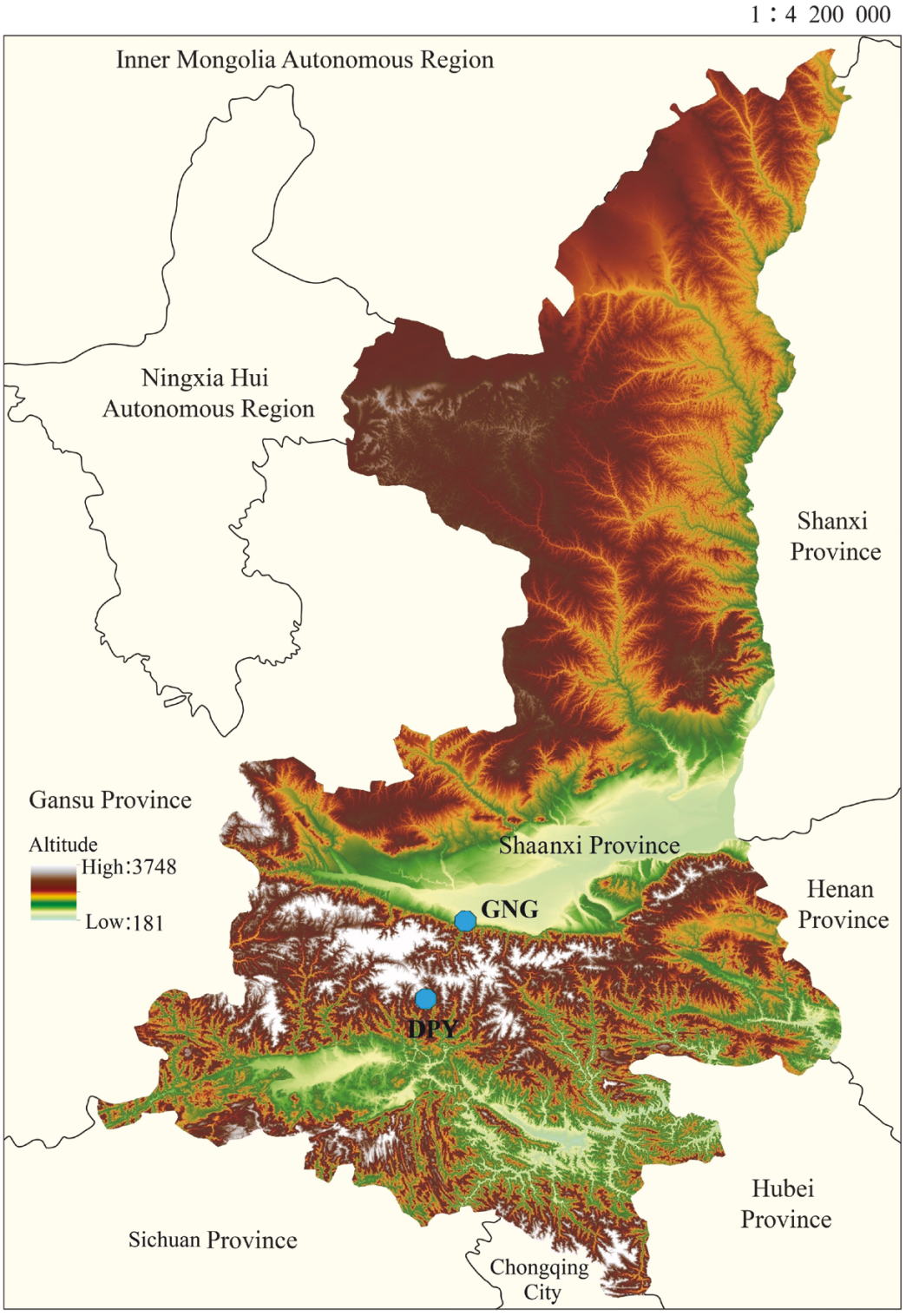

Figure 1. Location of the 2 *R. roxellana* populations (Shaanxi Province, China) used for this study (The Shaanxi Province map is downloaded from the Standard Map Service System at the website http://bzdt.ch.mnr.gov.cn/).

sequencing 12 clones for each individual. PCR reaction mix, amplification procedure, amplification products purification, and cloning of amplicons were conducted using previously described methods (Zhang et al. 2016). For *DRB1* and *DRB2* loci, we amplified 2 loci using a pair of primers and conducted amplicon-based next-generation sequencing (NGS). Each amplicon was amplified using barcode incorporation primers and purified using an AP-PCR-250 purification kit (AXYGEN). Purified products were quantified using a Qubit high-sensitivity kit and normalized to 10 ng/μL final concentration in a mixed amplicons library. The library was then sequenced on an Illumina NovaSeq 6000 platform using 250 bp pair-end reads at Beijing Novogene, Beijing, China.

Table 1. Summary of 2 study populations

Population	Sampling time	Population size	Samples	Sampled individuals
GNG	2012–2018	130–150 individuals	238 (193 hairs, 45 feces)	199
DPY	2015–2021	70–95 individual	163 (132 hairs, 31 feces)	107

Prior to each DNA extraction and polymerase chain reaction (PCR) process, the laboratory bench was washed with 75% ethanol. To avoid contamination with human DNA, all tools and consumables were sterilized with UV light for at least 30 min before each use. In addition, separate negative controls were incorporated for each PCR reaction.

Data analysis

Identification of MHC alleles and haplotype construction

For both traditional sequencing data (*DQA1* and *DQB1*) and NGS data (*DRB1* and *DRB2*), we defined any sequence as an allele if it was detected in at least 2 individuals. For NGS data, raw fastq files were managed using a described bioinformatics pipeline (Sommer et al. 2013; Santos et al. 2017; Zhang et al. 2023), which enables the separation of true alleles from artefacts. The work-flow consisted of the following 4 steps: 1) preparation of raw files for processing, 2) initial data quality check and reads filtering, 3) putative MHC alleles and artefacts identification, and finally 4) assignment of alleles to individuals (Sommer et al. 2013; Santos et al. 2017). MHC-TYPER V1.0 (Huang et al. 2019) was used to assign *DRB* alleles to a specific locus.

Next, linkage disequilibrium analysis and haplotype construction were performed using SHEsis software (http://analysis.bio-x.cn/myAnalysis.php; Shi and He 2005).

Genetic diversity of MHC and SSR

The level of genetic variation and polymorphism was calculated for MHC and SSR loci in both populations. The number of variable nucleotide sites (V_N), number of variable amino acid residues (V_{AA}), and polymorphism information content (*PIC*) of 4 MHC loci were obtained using MEGA V7.0 (Kumar et al. 2016). The per-site population mutation rate (θ_W) and per-site pairwise diversity (π) were calculated with DnaSP V6 (Rozas et al. 2017), using a Jukes–Cantor model of substitutions and standard errors calculated with 5,000 bootstrap replications. The deviation from the Hardy–Weinberg equilibrium (HWE) was calculated using CERVUS V3.0 (Kalinowski et al. 2007). Bonferroni correction was used to account for potential type I errors resulting from multiple tests for the 20 SSR loci. Expected heterozygosity (H_E), observed heterozygosity (H_O), inbreeding coefficient (F_{IS}) based on the minimum sample size and each locus, and the number of effective alleles (A_R) per locus of MHC and SSR were calculated with PolyGene (Huang et al. 2020).

Population differentiation

To analyze the genetic differentiation of the 2 populations, the *F* statistics (F_{ST}) of both MHC and SSR were calculated based on allele frequency using Genepop V4 (Rousset 2008). Principal coordinate analysis (PCoA) of the MHC and SSR data sets of the 2 populations was performed with GENALEX V6.5 (Peakall and Smouse 2012), and the PCoA scatter diagram was drawn using the R package ggplot2 V3.3.5 (https://github.com/tidyverse/ggplot2). The STRUCTURE V2.2.3 based on a Bayesian model was used to infer distinct grouping structures using SSR and MHC data for the 2 studied populations (Pritchard et al. 2000). The optimal number of populations was determined by DeltaK (ΔK), which was calculated using STRUCTURE HARVESTER (Evanno et al. 2005; Earl and Vonholdt 2012).

Migration and gene flow analysis

Historical gene flow (*Nm*) between the populations in both directions was estimated using MIGRATE-N V4.4.3 (Beerli 2006) based on SSR and MHC data sets. Recent migration rates (within 2–3 generations) between the 2 populations in both directions were estimated using a Bayesian method in BAYESASS V3.0 (Wilson and Rannala 2003).

Results

Genotyping and determining linked haplotypes

All samples from both populations were genotyped at 20 SSR loci. After individual identification using CERVUS V3.0, 306 non-repeating individuals (GNG: 199 individuals; DPY: 107 individuals) (Table 1) were detected and 287 individuals (GNG: 181 individuals; DPY: 106 individuals) were successfully genotyped for 4 MHC loci (*DQA1*, *DQB1*, *DRB1*, and *DRB2*) (Figure 2). In the 2 populations in total 4 *DRB2* alleles were detected, and for each of the other 3 loci 5 alleles were found, all alleles having been previously identified in other *R. roxellana* populations (Supplementary Table S1). The number and frequency of alleles for each MHC locus in each population are shown in Figure 2.

Each *Rhro-DQA1*, *-DQB1*, *-DRB1*, and *-DRB2* sequence was aligned with the whole genome sequence of *R. roxellana* (GenBank accession numbers: NC_044552). All 4 loci are located on chromosome 4 (Figure 3). By using SHEsis the *D'* values were found to all exceed 0.93 (Supplementary Figure S1), thus showing strong linkage disequilibrium among all 4 MHC loci. Finally, we identified 8 MHC haplotypes in all individuals (H01–H08) (Table 2), with 3 haplotypes (H01, H02, and H04) shared between both populations.

Diversity of MHC genes

The nucleotide and amino acid sequences of the 4 MHC loci were highly variable. The sequences of the 4 MHC loci differed at 27–36 of nucleotide positions (average = 32) in the DPY population and differed at 37–47 of nucleotide positions (average = 42) in the GNG population (Table 3). For the amino acid levels, the 4 MHC loci sequences differed at 14–24 of amino acid positions (average = 18.3) in DPY, whereas these loci sequences differed at 19–29 of amino acid positions (average = 23) in GNG (Table 3). The frequencies of all 4 MHC loci in both populations concurred with the expectations under HWE. The PIC, expected heterozygosity and observed heterozygosity of the GNG population all exceeded 0.5 (average $PIC = 0.62$, $H_E = 0.67$, $H_O = 0.72$), with the mean number of effective alleles (A_R) at 4 loci being 3.10 (Table 3). This showed high genetic polymorphism and high levels of heterozygosity in the GNG population. However, in the DPY population, the PIC, expected heterozygosity, and observed heterozygosity values were all lower than 0.5 (average $PIC = 0.42$, $H_E = 0.47$, $H_O = 0.47$), with the mean number

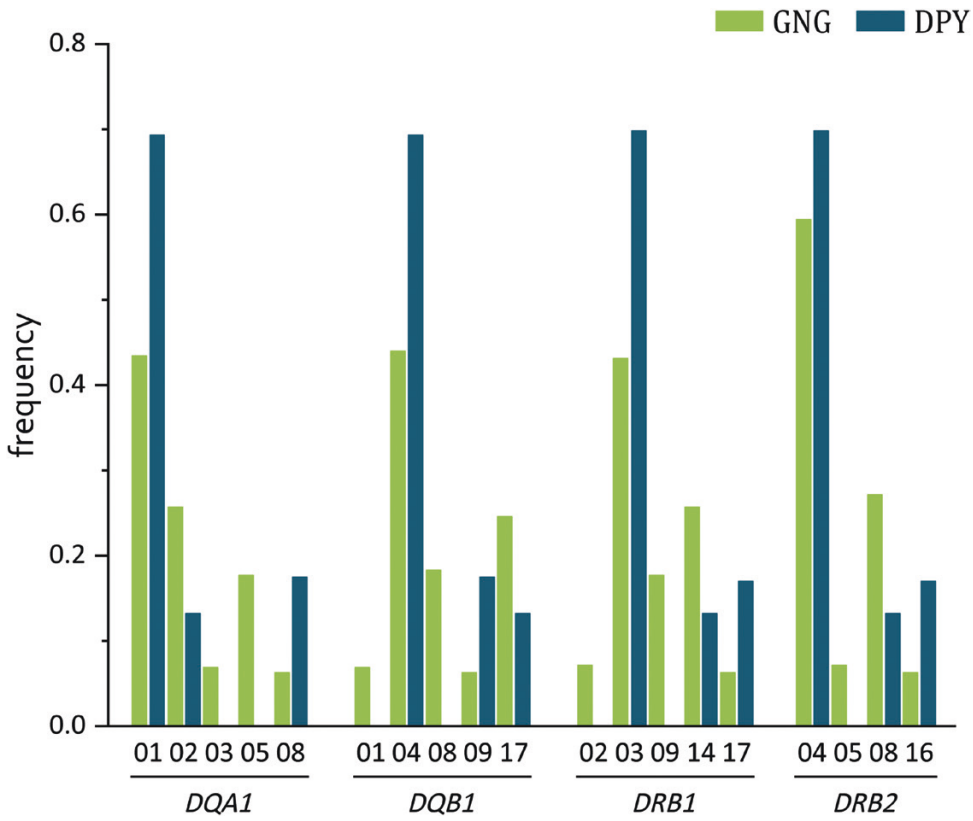

Figure 2. Allele frequencies of 4 MHC loci (*DQA1*, *DQB1*, *DRB1*, and *DRB2*) in 2 *Rhinopithecus roxellana* populations in the Qinling Mountains. The dark green and light green columns represent the DPY and the GNG population, respectively.

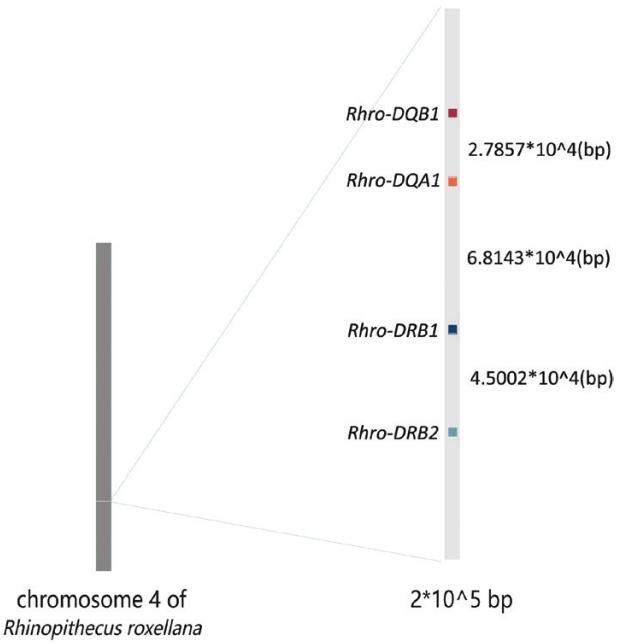

Figure 3. Relative location of 4 MHC class II genes investigated in this study within the full genomic region of *Rhinopithecus roxellana* on chromosome 4 (Wang et al. 2019).

of effective alleles at 4 loci was only 1.87 (Table 3). This showed moderate levels of polymorphism and heterozygosity in the DPY population. The genetic diversity levels of linked haplotypes in both populations almost equaled that of a single locus (GNG: *PIC* = 0.67; H_E = 0.72, H_O = 0.77, A_R = 3.52; DPY: *PIC* = 0.42, H_E = 0.46, H_O = 0.47, A_R = 1.87) (Table 3). Furthermore, nucleotide diversity was actually high for each MHC locus in both populations (GNG: π = 0.055–0.066, θ_W = 0.024–0.030; DPY: π = 0.028–0.043, θ_W = 0.019–0.025) suggesting that the alleles of these loci are highly divergent. The mean value of the inbreeding coefficient (F_{IS}) for MHC-linked haplotype was –0.053, indicating that there is little or no inbreeding in both *R. roxellana* populations (Table 5).

SSR diversity

After Bonferroni correction, we found no evidence that any SSR locus deviated from Hardy–Weinberg expectations. The GNG population showed high levels of both polymorphism (*PIC* = 0.50) and heterozygosity (H_E = 0.56, H_O = 0.57), with the mean number of effective alleles (A_R) at SSRs being 2.55 (Table 4). The DPY population showed moderate polymorphism (*PIC* = 0.46) and high heterozygosity (H_E = 0.53, H_O = 0.54), with the mean number of effective alleles (A_R) at SSRs being 2.30 (Table 4). The mean value of the F_{IS} for 20 SSRs was –0.015, indicating that there is little or no inbreeding in each of these *R. roxellana* populations (Table 5).

Population differentiation

Three methods were used to detect the differentiation between the 2 populations (DPY and GNG). First, we found that estimates of differentiation between the 2 populations were reduced when measured using adaptive MHC genes than for SSR (F_{ST}: MHC = 0.082, SSR = 0.163) (Table 5). Then, when using STRUCTURE V2.2.3, DeltaK reached a peak when *K* = 2 for both MHC and SSR. Both populations had mixed colors of MHC genes, showing that these 2 populations have

mixed genetic lineages (Figure 4). Differentiation is higher for SSR, showing almost uniform color for each of the 2 populations, indicating that both populations have a relatively pure genetic lineage for SSR. Finally, our PCoA analysis also showed high differentiation between populations for SSR, but this was not significant for MHC genes (Figure 5). In the PCoA scatter plot, the 95% confidence intervals for MHC genes of both populations overlap considerably, whereas for SSR there is complete segregation. Overall, the results of 3 different methods (F_{ST}, Structure, and PCoA) all showed that the differentiation of SSRs between the 2 populations is greater than that of MHC.

Gene flow between 2 populations

The recent gene flow of MHC between the 2 populations was significantly greater than that of SSR (Table 6). The recent migration rate of MHC genes from the DPY population to GNG population was more than 140 times that of the SSR population (MHC: 0.2513; SSR: 0.0017), and more than 20 times that in the opposite direction (MHC: 0.0833; SSR: 0.0031) (Table 6). For historical gene flow, the migration rate of both MHC and SSRs from the DPY population to the GNG population was higher than that in the opposite direction (MHC: DPY → GNG: 291.7 > GNG → DPY: 48.3; SSR: DPY → GNG: 211.0 > GNG → DPY: 94.3) (Table 6).

Table 2. Composition of *DQA1*, *DQB1*, *DRB1*, and *DRB2* linked haplotypes

Haplotype	Composition
H01	*DQA1*01~DQB1*04~DRB1*03~DRB2*04*
H02	*DQA1*02~DQB1*17~DRB1*14~DRB2*08*
H03	*DQA1*05~DQB1*08~DRB1*09~DRB2*04*
H04	*DQA1*08~DQB1*09~DRB1*17~DRB2*16*
H05	*DQA1*03~DQB1*01~DRB1*02~DRB2*05*
H06	*DQA1*05~DQB1*08~DRB1*09~DRB2*08*
H07	*DQA1*02~DQB1*08~DRB1*14~DRB2*08*
H08	*DQA1*02~DQB1*04~DRB1*14~DRB2*08*

Discussion

We measured genetic variation at 4 MHC loci and 20 SSRs in 2 wild *R. roxellana* populations (GNG and DPY). We detected 8 four-loci-linked haplotypes (01, 02, 03, 04, 05, 06, 07, and 08) formed by 5 *DQA1* alleles, 5 *DQB1* alleles, 5 *DRB1* alleles, and 4 *DRB2* alleles. The GNG population showed high genetic polymorphism and high levels of heterozygosity in both MHC and SSR (MHC: *PIC* = 0.67, H_E = 0.72; SSR: *PIC* = 0.50, H_E = 0.56) (Table 3), while the DPY population showed moderate levels of diversity and heterozygosity in MHC, and moderate levels of diversity and high levels of heterozygosity in SSR (MHC: *PIC* = 0.42, H_E = 0.47; SSR: *PIC* = 0.46, H_E = 0.53) (Table 3). The genetic diversity of *R. roxellana* is lower than that of the rhesus macaque *M. mulatta*, which in China has a population size 5 times larger than *R. roxellana* (Liu et al. 2018). For example, there are 23 *MHC-DQB1* alleles and a higher level of *DQB1* heterozygosity (H_E > 0.71) in 5 wild *M. mulatta* populations in the west of Sichuan province in China (Yao et al. 2014). The genetic diversity of *R. roxellana* is also lower than that of a wild chacma baboon *Papio ursinus* population in Tsaobis Leopard Park in Southern Africa, which has 16 different *MHC-DRB* sequences and higher heterozygosity (0.83) (Huchard et al. 2006, 2010). Such differences may be due to *M. mulatta and P. ursinus* having wider distributions, larger population sizes, and occupying more wider ecological niches than *R. roxellana*

Table 3. Genetic diversity of 4 MHC loci and their linked haplotypes (*DQA1*, *DQB1*, *DRB1*, and *DRB2*) in the 2 study populations

Population	Locus	V_N	V_{AA}	*PIC*	H_E	H_O	A_R	π	θ_W
DPY	*DQA1*	30	16	0.42	0.47	0.47	1.87	0.028	0.021
	DQB1	35	19	0.42	0.47	0.47	1.87	0.037	0.023
	DRB1	36	24	0.42	0.47	0.47	1.87	0.043	0.025
	DRB2	27	14	0.42	0.47	0.47	1.87	0.043	0.019
	Mean of 4 genes	32	18	0.42	0.47	0.47	1.87	0.038	0.022
	Linked haplotype	128	73	0.42	0.47	0.47	1.87	0.038	0.022
GNG	*DQA1*	43	23	0.66	0.70	0.77	3.38	0.066	0.027
	DQB1	41	21	0.66	0.70	0.76	3.37	0.064	0.025
	DRB1	47	29	0.66	0.70	0.77	3.38	0.065	0.030
	DRB2	37	19	0.50	0.56	0.57	2.26	0.055	0.024
	Mean of 4 genes	42	23	0.62	0.67	0.72	3.10	0.063	0.027
	Linked haplotype	168	92	0.67	0.72	0.77	3.52	0.062	0.026
Total	*DQA1*	43	23	0.61	0.65	0.66	2.84	0.059	0.025
	DQB1	41	21	0.60	0.65	0.66	2.83	0.060	0.023
	DRB1	47	29	0.61	0.65	0.66	2.84	0.060	0.028
	DRB2	37	19	0.48	0.53	0.53	2.15	0.051	0.022
	Mean of 4 genes	42	23	0.57	0.62	0.63	2.66	0.058	0.025
	Linked haplotype	168	92	0.61	0.65	0.66	2.88	0.058	0.025

V_N, number of variable nucleotide sites; V_{AA}, number of variable amino acid residues; *PIC*, the polymorphism information content; H_E, expected heterozygosity; H_O, observed heterozygosity; A_R, effective alleles; π, per site pairwise nucleotide diversity; θ_W, per site population mutation rate.

(Oldenbroek 2007; Vangenot et al. 2020). However, the giant panda, *Ailuropoda melanoleuca*, a species that inhabits much the same habitat and thus has a similar distribution to *R. roxellana* (National Forestry and Grassland Administration 2015; Zhao et al. 2018) has similar levels of genetic diversity (MHC: H_E = 0.44–0.71) to *R. roxellana* (Zhang et al. 2015), even though it is a solitary mammal. In addition, some other endangered vertebrate species have lower levels of MHC diversity than *R. roxellana* and may be the result of more severe habitat degradation and loss, faster population declines, lower rates of gene flow among populations, and stronger genetic drift within populations. For example, in 7 relict European and Asian beaver *Castor fiber* populations *DRB* diversity in 6 populations had become fixed to a unique allele, with only one population being polymorphic and containing 4 alleles, which may have resulted from superimposition of a bottleneck on preexisting genetic structure due to population subdivision (Babik et al. 2005). In African wild dogs *Lycaon pictus*, the *DLA–DQA1* locus and the *DLA–DQB1* locus are monomorphic and dimorphic, respectively, due to extensive population bottlenecks and population declines (Marsden et al. 2009). Overall, population demographic history, habitat range, habitat diversity, and population structure shaped the level of genetic diversity of different species.

Table 4. Genetic diversity of 20 SSRs of the 2 study populations (DPY and GNG)

Population	N_A	*PIC*	H_E	H_O	A_R
GNG	5.75	0.50	0.56	0.57	2.55
DPY	4.40	0.46	0.53	0.54	2.30
Total	7.00	0.54	0.60	0.56	2.74

N_A, average number of alleles; *PIC*, the polymorphism information content; H_E, expected heterozygosity; H_O, observed heterozygosity; A_R, effective alleles.

Table 5. Summary of *F*-statistics and G_{ST} for 4 MHC genes linked haplotype and SSR of the 2 study populations (DPY and GNG)

Gene	F_{IS}	F_{IT}	F_{ST}
MHC	–0.053	0.034	0.082
SSR	–0.015	0.150	0.163

F_{IS}, inbreeding coefficient within individuals; F_{IT}, mean inbreeding coefficient within 2 populations; F_{ST}, inbreeding coefficient within populations.

In the present study, we found that the DPY population has fewer alleles for each MHC locus and fewer linked haplotypes than the GNG population (DPY: 12 alleles formed 3 haplotypes; GNG: 19 alleles formed 8 haplotypes) (Figure 2 and Table 3). Each allele for haplotype H08 also occurs in the DPY population. However, these alleles formed H01 and H02, rather than H08 (a recon of H01 and H02 with one time of crossover) in DPY. Due to our use of deep sampling, the probability of missing H08 was low, but it cannot be excluded that H08 exists in offspring within the DPY population. The DPY population losing some MHC alleles and haplotypes may be due to at least 3 factors. First, the population size of DPY is only about half of that of the GNG population (Table 1). Compared with the GNG population, the DPY population is thus likely to be at greater risk of allele loss and genetic variation reduction due to genetic drift (Ouborg et al. 2010) (Arroyo-Rodriguez and Dias 2010; Ouborg et al. 2010; Rosas et al. 2011; Luo et al. 2012b). Second, there is significant divergence between the DPY and its neighbor population (F_{ST} = 0.034, P < 0.05; Huang et al. 2016); while the GNG population shows little divergence with its neighbor

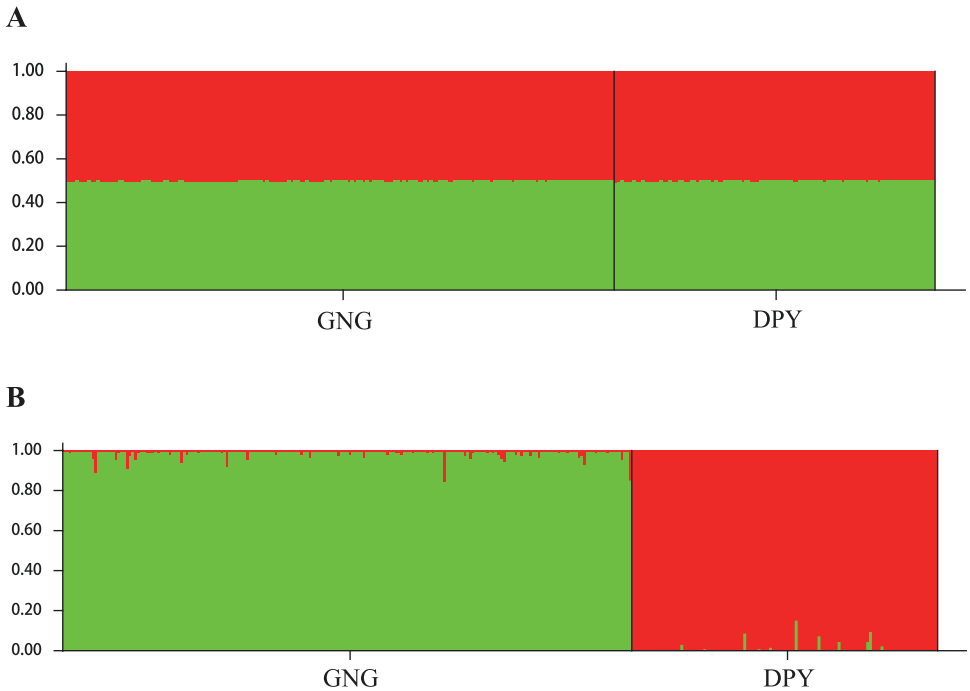

Figure 4. Structure analysis for MHC (A) and SSR (B) genes. Bar plots for K = 2. Results of the run with the highest value of LnPD were used.

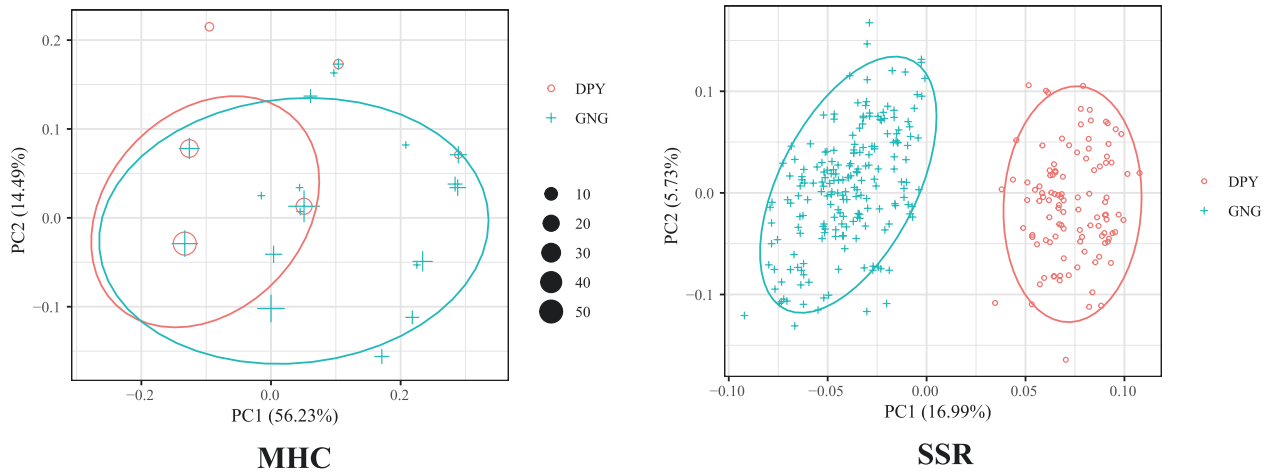

Figure 5. Principal coordinates analysis (PCoA) results.

Table 6. Estimates of recent migration rate (M) and historical immigrants per generation (*N*m) between the 2 study populations

Software	Marker	GNG → DPY	DPY → GNG
Migrate-*n* (Nm)	MHC	48.3 (14.7–98.7)[a]	291.7 (229.3–442.0)
	SSR	94.3 (87.3–94.6)	211.0 (210.0–231.3)
BAYESASS (M)	MHC	0.0833	0.2513
	SSR	0.0031	0.0017

[a]Values in parentheses brackets represented the 2.5–97.5% CI.

population (F_{ST} = 0.003, P > 0.05; Huang et al. 2016). This suggests the GNG population may have more gene flow with its neighbor population than that of the DPY population. Moreover, the GNG population has been reported to experience periodic fission–fusion events (individuals merge together to form a large population and then split into discrete smaller populations) with neighboring populations (Qi et al. 2014). The GNG and its neighboring populations may, therefore, exchange individuals during such events to promote gene flow among populations, which may help maintain a higher level of genetic variation in the GNG population (Qu et al.1993; Savage and Baker 1996; Li et al. 2020). Finally, the mountain slope inhabited by the DPY population experienced a greater degree of deforestation and hence habitat fragmentation during the 1950s–1980s than the slope inhabited by the GNG population (Yang et al. 2016). Because *R. roxellana* is largely arboreal, this species has clearly been negatively affected over the last few decades by deforestation. Population isolation due to increased habitat fragmentation on the slope where the DPY population resides is may thus have decreased individual migration and gene flow than on the slope with more intact forest inhabited by the GNG population. Thus, it is most likely that the DPY population possesses fewer MHC alleles due to its smaller population size and lower gene flow with its neighboring populations.

The results of all 3 different methods (F_{ST}, structure, and PCoA) showed lower genetic differentiation in the MHC measurements than SSRs, suggesting that pathogen-mediated balancing selection may have homogenized the MHC genes in the 2 populations, which is consistent with previous research (Luo et al. 2012b; Song et al. 2016; Zhang et al. 2018). Balancing selection tends to maintain genetic variation within a population and can reduce the likelihood of population divergence when different populations each experience homogeneous selection pressures such as similar pathogens (Kubota and Watanabe 2013). Several other vertebrate species also have lower levels of genetic differentiation in MHC genes than neutral loci, such as Chinese alligators *A. sinensis*, domestic cats *Felis silvestris catu*, domestic goats *Capra hircus*, and guppies *Poecilia reticulata* (Fraser and Neff 2010; Morris et al. 2014; Zhai et al. 2017; Gong et al. 2021; Herdegen-Radwan et al. 2021). Nevertheless, opposite trends are present in golden pheasants *Chrysolophus pictus*, crested ibises *Nipponia nippon*, chinook salmon *Oncorhynchus tshawytscha*, and northern leopard frogs *Rana pipiens*, where levels of divergence of MHC genes exceed those of neutral genes among populations (Evans et al. 2010; He et al. 2017; Lan et al. 2019; Trujillo et al. 2021), which can be attributed to disruptive selection for local adaptations (Aguilar and Garza 2006; Awadi et al. 2018). Balancing selection and local adaptation thus have the potential to shape patterns of divergence of MHC genes among populations (Hansen et al. 2007; Cortázar-Chinarro et al. 2017). In any specific study, the dominant process requires identification. Based on lower genetic differentiation in MHC genes than SSRs, we conclude that balancing selection, rather than local adaptation, shapes genetic differentiation of MHC genes between the 2 *R. roxellana* populations (Ashby and Boots 2017).

Recent gene flow also supports balancing selection for MHC genes. In recent generations, gene flow measured by MHC genes was higher than when measured by SSRs (27 fold from GNG to DPY, 148 fold from DPY to GNG), may reflect reduced differentiation between the 2 populations at MHC genes resulting from balancing selection (Table 6).

In conclusion, we investigated genetic variation, population differentiation, and gene flow of 2 wild *R. roxellana* populations using adaptive MHC genes and neutral SSRs. Overall, we found a higher level of genetic diversity in the larger GNG population compared with the smaller DPY population, and evidence that patterns of differentiation for MHC genes between the 2 populations are shaped by balancing selection rather than local adaptation. Follow-up studies using more MHC loci and expanding the geographical scale will likely improve knowledge of the conservation genetics of this species. Our study provides a better understanding of

the effects of balancing selection and genetic drift in small and fragmented populations, and additional genetic data for conservation of similar vertebrate populations in the absence of long-distance migration.

Author Contributions

P.Z. and B.G.L. designed this research. S.X.D., B.Y.Z., F.N., M.J.Y., H.Y.H., Y.Y.Z., J.B.Y., Y.N.L., and J.Q.L. contributed to sample and data collection in the field and carried out the molecular genetic studies. S.X.D., K.H., and P.Z. establish the model and analyzed the data. S.X.D. wrote the manuscript, with help from P.Z., Y.R., D.W.D., and other authors.

Acknowledgements

We thank the staff of the Shaanxi Key Laboratory of Animal Conservation for the samples provided and field assistance. We also thank He Zhang for drawing the map of the study populations.

Funding

This study was funded by the Strategic Priority Research Program of the Chinese Academy of Sciences (XDB31020302), the National Natural Science Foundation of China (31730104, 31770425, 32071495, 32170515, 32070453, and 32000317). Derek W. Dunn was supported by a Shaanxi Province Talents 100 Fellowships.

Conflict of Interest

The authors declare that they have no conflict of interest.

Supplementary Material

Supplementary material can be found at https://academic.oup.com/cz.

References

Aguilar A, Garza JC, 2006. A comparison of variability and population structure for major histocompatibility complex and microsatellite loci in California coastal steelhead *Oncorhynchus mykiss Walbaum*. *Mol Ecol* **15**(4):923–937.

Allen M, Engstrom AS, Meyers S, Handt O, Saldeen T et al., 1998. Mitochondrial DNA sequencing of shed hairs and saliva on robbery caps: Sensitivity and matching probabilities. *J Forensic Sci* **43**(3):453–464.

Arroyo-Rodriguez V, Dias PA, 2010. Effects of habitat fragmentation and disturbance on howler monkeys: A review. *Am J Primatol* **72**(1):1–16.

Ashby B, Boots M, 2017. Multi-mode fluctuating selection in host-parasite coevolution. *Ecology Lett* **20**(3):357–365.

Awadi A, Ben Slimen H, Smith S, Steve S, Felix K et al., 2018. Positive selection and climatic effects on MHC class II gene diversity in hares *Lepus capensis* from a steep ecological gradient. *Sci Rep* **8**:11514.

Babik W, Durka W, Radwan J, 2005. Sequence diversity of the MHC DRB gene in the Eurasian beaver *Castor fiber*. *Mol Ecol* **14**(14):4249–4257.

Beerli P, 2006. Comparison of Bayesian and maximum-likelihood inference of population genetic parameters. *Bioinformatics* **22**(3):341–345.

Boyd RJ, Denomme MR, Grieves LA, Elizabeth A, 2021. Stronger population differentiation at infection-sensing than infection-clearing innate immune loci in songbirds: Different selective regimes for different defenses. *Evolution* **75**(11):2736–2746.

Cortázar-Chinarro M, Lattenkamp EZ, Meyer-Lucht Y, Luquet E, Laurila A et al., 2017. Drift, selection, or migration? Processes affecting genetic differentiation and variation along a latitudinal gradient in an amphibian. *BMC Evol Biol* **17**:189.

Courchamp F, Berec J, Gascoigne J, 2008. *Allee Effects in Ecology and Conservation*. New York: Oxford University Press.

Courchamp F, Clutton-Brock T, Grenfell B, 1999. Inverse density dependence and the Allee effect. *Trends Ecol Evol* **14**(10):405–410.

de Groot NG, de Groot N, de Vos-Rouweler AJM, Louwerse A, Bruijnesteijn J et al., 2022. Dynamic evolution of MHC haplotypes in cynomolgus macaques of different geographic origins. *Immunogenetics* **74**(4):409–429.

Earl DA, Vonholdt BM, 2012. STRUCTURE HARVESTER: A website and program for visualizing STRUCTURE output and implementing the Evanno method. *Conserv Genet Resour* **4**(2):359–361.

Eizaguirre C, Lenz TL, Kalbe M, Milinski M, 2012. Rapid and adaptive evolution of MHC genes under parasite selection in experimental vertebrate populations. *Nat Commun* **3**:621.

Evanno G, Regnaut S, Goudet J, 2005. Detecting the number of clusters of individuals using the software STRUCTURE: A simulation study. *Mol Ecol* **14**(8):2611–2620.

Evans ML, Neff BD, Heath DD, 2010. MHC genetic structure and divergence across populations of chinook salmon *Oncorhynchus tshawytscha*. *Heredity* **104**(5):449–459.

Fitzpatrick SW, Bradburd GS, Kremer CT, Patricia ES, Lisa MA et al., 2020. Genomic and fitness consequences of genetic rescue in wild populations. *Curr Biol* **30**(3):517–522.e5.

Fraser BA, Neff BD, 2010. Parasite mediated homogenizing selection at the MHC in guppies. *Genetica* **138**(2):273–278.

Gong Y, Guo Y, He YM, Yuan BG, Yang XH et al., 2021. Comparative analysis of the genetic diversity of the neutral microsatellite loci and second exon of the goat MHC-DQB1 gene. *Anim Biotechnol* **34**(1):85–92.

Haimoff EH, Yang XJ, He SJ, Chen N, 1987. Preliminary observations of wild black-crested gibbons *Hylobates concolor concolor* in Yunnan province, people's republic of China. *Primates* **28**(3):319–335.

Hansen MM, Skaala O, Jensen LF, Bekkevold D, Karen-Lise D et al., 2007. Gene flow, effective population size and selection at major histocompatibility complex genes: Brown trout in the Hardanger Fjord, Norway. *Mol Ecol* **16**(7):1413–1425.

He K, Liang CH, Zhu Y, Dunn P, Zhao A et al., 2022a. Reconstructing macroevolutionary patterns in avian MHC architecture with genomic data. *Front Genet* **13**:868236.

He K, Liu HY, Ge YF, Wu SY, Wan QH, 2017. Historical gene flow and profound spatial genetic structure among golden pheasant populations suggested by multi-locus analysis. *Mol Phylogenet Evol* **110**:93–103.

He K, Zhu Y, Yang SC, Ye Q, Fang SG et al., 2022b. Major histocompatibility complex genomic investigation of endangered Chinese alligator provides insights into the evolution of tetrapod major histocompatibility complex and survival of critically bottlenecked species. *Frontiers Ecol Evol* **10**:1078058.

Herdegen-Radwan M, Phillips KP, Babik W, Mohammed RS, Radwan J, 2021. Balancing selection versus allele and supertype turnover in MHC class II genes in guppies. *Heredity* **126**(3):548–560.

Hoffman AM, Bushey JA, Ocheltree TW, Smit MD, 2020. Genetic and functional variation across regional and local scales is associated with climate in a foundational prairie grass. *New Phytol* **227**(2):352–364.

Huang K, Dunn DW, Ritland K, Li BG, 2020. POLYGENE: Population genetics analyses for autopolyploids based on allelic phenotypes. *Methods Ecol Evol* **11**(3):448–456.

Huang K, Guo ST, Cushman SA, Dunn DW, Qi XG et al., 2016. Population structure of the golden snub-nosed monkey

Rhinopithecus roxellana in the Qinling Mountains, central China. *Integr Zool* **11**(5):350–360.
Huang K, Zhang P, Dunn DW, Wang TC, Mi R et al., 2019. Assigning alleles to different loci in amplifications of duplicated loci. *Mol Ecol Resour* **19**(5):1240–1253.
Huchard E, Alvergne A, Féjan D, Knapp LA, Cowlishaw G et al., 2010. More than friends? Behavioural and genetic aspects of heterosexual associations in wild chacma baboons. *Behav Ecol Sociobiol* **64**:769–781.
Huchard E, Cowlishaw G, Raymond M, Weill M, Knapp LA, 2006. Molecular study of Mhc-DRB in wild chacma baboons reveals high variability and evidence for trans-species inheritance. *Immunogenetics* **58**:805–816.
Kalinowski ST, Taper ML, Marshall TC, 2007. Revising how the computer program CERVUS accommodates genotyping error increases success in paternity assignment. *Mol Ecol* **16**(5):1099–1106.
Kaufmann J, Lenz TL, Kalbe M, Milinski M, Eizaguirre C, 2017. A field reciprocal transplant experiment reveals asymmetric costs of migration between lake and river ecotypes of three-spined sticklebacks *Gasterosteus aculeatus*. *J Evol Biol* **30**(5):938–950.
Klein J, 1987. Origin of major histocompatibility complex polymorphism: The trans-species hypothesis. *Hum Immunol* **19**(3):155–162.
Kubota H, Watanabe K, 2013. Loss of genetic diversity at an MHC locus in the endangered Tokyo bitterling Tanakia tanago (Teleostei: Cyprinidae). *Zool Sci* **30**(12):1092–1101.
Kumar S, Stecher G, Tamura K, 2016. MEGA7: Molecular evolutionary genetics analysis version 7.0 for bigger datasets. *Mol Biol Evol* **33**(7):1870–1874.
Lan H, Zhou T, Wan QH, Fang SG, 2019. Genetic diversity and differentiation at structurally varying MHC haplotypes and microsatellites in bottlenecked populations of endangered crested ibis. *Cells* **8**(4):377.
Li BG, Pan RL, Oxnard CE, 2002. Extinction of snub-nosed monkeys in China during the past 400 years. *Int J Primatol* **23**(6):1227–1244.
Li YL, Wang L, Wu JW, Ye XP, Garber PA et al., 2020. Bachelor groups in primate multilevel society facilitate gene flow across fragmented habitats. *Curr Zool* **66**(2):113–122.
Liu ZJ, Tan XX, Orozco-terWengel P, Zhou XM, Zhang LY et al., 2018. Population genomics of wild Chinese rhesus macaques reveals a dynamic demographic history and local adaptation, with implications for biomedical research. *GigaScience* **7**(9):giy106.
Long YC, Richardson M, 2021. *Rhinopithecus roxellana* (amended version of 2020 assessment). *The IUCN Red List of Threatened Species* **2021**:e.T19596A196491153. Available from: https://www.iucnredlist.org/species/19596/196491153.
Luo MF, Liu ZJ, Pan HJ, Zhao L, Li M, 2012a. Historical geographic dispersal of the golden snub-nosed monkey *Rhinopithecus roxellana* and the influence of climatic oscillations. *Am J Primatol* **74**(2):91–101.
Luo MF, Pan HJ, 2013. MHC II DRB variation and trans-species polymorphism in the golden snub-nosed monkey *Rhinopithecus roxellana*. *Chin Sci Bull* **58**(18):2119–2127.
Luo MF, Pan HJ, Liu ZJ, Li M, 2012b. Balancing selection and genetic drift at major histocompatibility complex class II genes in isolated populations of golden snub-nosed monkey *Rhinopithecus roxellana*. *BMC Evol Biol* **12**:207.
Manel S, Guerin PE, Mouillot D, Blanchet S, Velez L et al., 2020. Global determinants of freshwater and marine fish genetic diversity. *Nat Commun* **11**:692.
Marsden CD, Mable BK, Woodroffe R, Rasmussen GSA, Cleaveland S et al., 2009. Highly endangered African wild dogs *Lycaon pictus* lack variation at the major histocompatibility complex. *J Hered* **100**(suppl_1):S54–S65.
Moqanaki EM, Cushman SA, 2017. All roads lead to Iran: Predicting landscape connectivity of the last stronghold for the critically endangered Asiatic cheetah. *Anim Conserv* **20**(1):29–41.
Morris AB, Ickert-Bond SM, Brunson DB, Soltis DE, Soltis PS, 2008. Phylogeographical structure and temporal complexity in American sweetgum (*Liquidambar styraciflua*; Altingiaceae). *Mol Ecol* **17**(17):3889–3900.
Morris KM, Kirby K, Beatty JA, Barrs VR, Cattley S et al., 2014. Development of MHC-linked microsatellite markers in the domestic cat and their use to evaluate MHC diversity in domestic cats, cheetahs, and Gir lions. *J Hered* **105**:493–505.
Nabutanyi P, Wittmann MJ, 2021. Models for eco-evolutionary extinction vortices under balancing selection. *Am Naturalist* **197**(3):336–350.
National Forestry and Grassland Administration, 2015. *The Fourth National Survey Report on Giant Panda in China*. Beijing: China Science Publishing & Media Ltd.
Neefjes J, Jongsma MLM, Paul P, Bakke O, 2011. Towards a systems understanding of MHC class I and MHC class II antigen presentation. *Nat Rev Immunol* **11**(12):823–836.
Oldenbroek JK, 2007. Utilisation and conservation of farm animal genetic resources. *Embo J* **17**(22):6573–6586.
Ouborg NJ, Pertoldi C, Loeschcke V, Bijlsma RK, Hedrick PW, 2010. Conservation genetics in transition to conservation genomics. *Trends Genetics* **26**(4):177–187.
Paterson NM, Al-Zubieri H, Barber MF, 2021. Diversification of CD1 molecules shapes lipid antigen selectivity. *Mol Biol Evol* **38**(6):2273–2284.
Peakall R, Smouse PE, 2012. GenAlEx 6.5: Genetic analysis in Excel. Population genetic software for teaching and research-an update. *Bioinformatics* **28**(19):2537–2539.
Potter KM, Campbell AR, Josserand SA, Nelson CD, Jetton RM, 2017. Population isolation results in unexpectedly high differentiation in Carolina hemlock *Tsuga caroliniana*, an imperiled southern Appalachian endemic conifer. *Tree Genet Genomes* **13**(5):105.
Princepe D, de Aguiar MAM, Plotkin JB, 2022. Mito-nuclear selection induces a trade-off between species ecological dominance and evolutionary lifespan. *Nat Ecol Evol* **6**(12):1992–2002.
Pritchard JK, Stephens M, Donnelly P, 2000. Inference of population structure using multilocus genotype data. *Genetics* **155**(2):945–959.
Qi XG, Garber PA, Ji WH, Huang ZP, Huang K et al., 2014. Satellite telemetry and social modeling offer new insights into the origin of primate multilevel societies. *Nat Commun* **5**:5296.
Qi XG, Huang K, Fang G, Grueter CC, Dunn DW et al., 2017. Male cooperation for breeding opportunities contributes to the evolution of multilevel societies. *Proc Biol Sci* **284**(1863):20171480.
Qi XG, Li BG, Garber PA, Ji WH, Watanabe K, 2009. Social dynamics of the golden snub-nosed monkey *Rhinopithecus roxellana*: Female transfer and one-male unit succession. *Am J Primatol* **71**(8):670–679.
Qiu CL, Yang GB, Yu K, Li LL, Liu Q et al., 2008. Characterization of the major histocompatibility complex class II DQB (*MhcMamu-DQB1*) alleles in a cohort of Chinese rhesus macaques *Macaca mulatta*. *Hum Immunol* **69**(8):513–521.
Qu WY, Zhang YZ, David M, Southwick CH, 1993. Rhesus monkeys *Macaca mulatta* in the Taihang mountains. *Int J Primatol* **14**(4):607–621.
Rosas F, Quesada M, Lobo JA, Sork VL, 2011. Effects of habitat fragmentation on pollen flow and genetic diversity of the endangered tropical tree *Swietenia humilis* (Meliaceae). *Biol Conserv* **144**(12):3082–3088.
Rousset F, 2008. Genepop'007: A complete reimplementation of the Genepop software for Windows and Linux. *Mol Ecol Resour* **8**(1):103–106.
Rozas J, Ferrer-Mata A, Sánchez-DelBarrio JC, Guirao-Rico S, Librado P et al., 2017. DnaSP 6: DNA sequence polymorphism analysis of large data sets. *Mol Biol Evol* **34**(12):3299–3302.
Ryan SO, Cobb BA, 2012. Roles for major histocompatibility complex glycosylation in immune function. *Semin Immunopathol* **34**(3):425–441.
Santos PSC, Michler FU, Sommer S, 2017. Can MHC-assortative partner choice promote offspring diversity? A new combination of

MHC-dependent behaviours among sexes in a highly successful invasive mammal. *Mol Ecol* **26**(8):2392–2404.

Satake A, Nagahama A, Sasaki E, 2022. A cross-scale approach to unravel the molecular basis of plant phenology in temperate and tropical climates. *New Phytol* **233**(6):2340–2353.

Savage A, Baker AJ, 1996. Callitrichid social structure and mating system: Evidence from field studies. *Am J Primatol* **38**(1):1–3.

Schierup MH, Charlesworth D, Vekemans X, 2000. The effect of hitch-hiking on genes linked to a balanced polymorphism in a subdivided population. *Genet Res* **76**(1):63–73.

Shi YY, He L, 2005. SHEsis, a powerful software platform for analyses of linkage disequilibrium, haplotype construction, and genetic association at polymorphism loci. *Cell Res* **15**(2):97–98.

Shortreed CG, Wiseman RW, Karl JA, Bussan HE, Baker DA et al., 2020. Characterization of 100 extended major histocompatibility complex haplotypes in Indonesian cynomolgus macaques. *Immunogenetics* **72**(4):225–239.

Slatkin M, 1987. Gene flow and the geographic structure of natural populations. *Science* **236**(4803):787–792.

Sommer S, Courtiol A, Mazzoni CJ, 2013. MHC genotyping of non-model organisms using next-generation sequencing: A new methodology to deal with artefacts and allelic dropout. *BMC Genomics* **14**:542.

Song XY, Zhang P, Huang K, Chen D, Guo ST et al., 2016. The influence of positive selection and trans-species evolution on *DPB* diversity in the golden snub-nosed monkeys *Rhinopithecus roxellana*. *Primates* **57**(4):489–499.

Trujillo AL, Hoffman EA, Becker CG, Savage AE, 2021. Spatiotemporal adaptive evolution of an MHC immune gene in a frog-fungus disease system. *Heredity* **126**(4):640–655.

Vangenot C, Nunes JM, Doxiadis GM, Poloni ES, Bontrop RE et al., 2020. Similar patterns of genetic diversity and linkage disequilibrium in Western chimpanzees Pan troglodytes verus and humans indicate highly conserved mechanisms of MHC molecular evolution. *BMC Evol Biol* **20**(1):119.

Wang BC, Zhu FZ, Shi ZC, Huang ZY, Sun RH et al., 2022. Molecular characteristics, polymorphism and expression analysis of MHC II in yellow catfish *Pelteobagrus fulvidraco* responding to *Flavobacterium columnare* infection. *Fish Shellfish Immunol* **125**:90–100.

Wang L, Wu JW, Liu XM, Di DD, Liang YH et al., 2019. A high-quality genome assembly for the endangered golden snub-nosed monkey *Rhinopithecus roxellana*. *GigaScience* **8**(8):1–11.

Weeks BC, Naeem S, Lasky JR, Tobias JA, 2022. Diversity and extinction risk are inversely related at a global scale. *Ecol Lett* **25**(3):697–707.

Willi Y, Van Buskirk J, Hoffmann AA, 2006. Limits to the adaptive potential of small populations. *Annu Rev Ecol Evol Syst* **37**:433–458.

Wilson GA, Rannala B, 2003. Bayesian inference of recent migration rates using multilocus genotypes. *Genetics* **163**(3):1177–1191.

Wittmann MJ, Stuis H, Metzler D, 2018. Genetic Allee effects and their interaction with ecological Allee effects. *J Anim Ecol* **87**(3):11–23.

Wolfert MA, Boons GJ, 2013. Adaptive immune activation: Glycosylation does matter. *Nat Chem Biol* **9**(12):776–784.

Xu SX, Ren WH, Li SZ, Wei FW, Zhou KY et al., 2009. Sequence polymorphism and evolution of three cetacean MHC genes. *J Mol Evol* **69**(3):260–275.

Yang QL, Huang XY, Zhao SG, Liu LX, Zhang SW et al., 2016. Effect of swine leukocyte antigen-DQA gene variation on diarrhea in Large White, Landrace, and Duroc piglets. *Anim Genet* **47**(6):691–697.

Yang X, Berman CM, Hu HY, Hou R, Huang K et al., 2022. Female preferences for male golden snub-nosed monkeys vary with male age and social context. *Curr Zool* **68**(2):133–142.

Yao YF, Dai QX, Li J, Ni QY, Zhang MW et al., 2014. Genetic diversity and differentiation of the rhesus macaque *Macaca mulatta* population in western Sichuan, China, based on the second exon of the major histocompatibility complex class II DQB (*MhcMamu*-DQB1) alleles. *BMC Evol Biol* **14**(1):1–13.

Zhai DD, Li WJ, Liu HZ, Cao WX, Gao X, 2019. Genetic diversity and temporal changes of an endemic cyprinid fish species, *Ancherythroculter nigrocauda*, from the upper reaches of Yangtze River. *Zool Res* **40**(5):427–438.

Zhai T, Yang HQ, Zhang RC, Fang LM, Zhong GH et al., 2017. Effects of population bottleneck and balancing selection on the Chinese alligator are revealed by locus-specific characterization of MHC genes. *Sci Rep* **7**:5549.

Zhang L, Wu Q, Hu Y, Wu H, Wei F, 2015. Major histocompatibility complex alleles associated with parasite susceptibility in wild giant pandas. *Heredity* **114**(1):85–93.

Zhang P, Huang K, Zhang BY, Dunn DW, Chen D et al., 2018. High polymorphism in *MHC-DRB* genes in golden snub-nosed monkeys reveals balancing selection in small, isolated populations. *BMC Evol Biol* **18**(1):29.

Zhang P, Song XY, Dunn DW, Huang K, Pan RL et al., 2016. Diversity at two genetic loci associated with the major histocompatibility complex in the golden snub-nosed monkey *Rhinopithecus roxellana*. *Biochem Syst Ecol* **68**:243–249.

Zhang P, Zhang BY, Dunn DW, Song XY, Huang K et al., 2023. Social and paternal female choice for male MHC genes in golden snub-nosed monkeys *Rhinopithecus roxellana*. *Mol Ecol* **32**:3239–3256.

Zhao XM, Ren BP, Garber PA, Li XH, Li M, 2018. Impacts of human activity and climate change on the distribution of snub-nosed monkeys in China during the past 2000 years. *Divers Distrib* **24**(1):92–102.